Fluorescent Pyrene Derivative of Concanavalin A: Preparation and Spectroscopic Characterization†

Brian A. Herman‡ and Salvador M. Fernandez*

ABSTRACT: The preparation and characterization of a fluorescent 1-pyreneacrylate–concanavalin A conjugate are described. Excitation, emission, and polarization spectra are presented as well as quantum yield and fluorescence lifetimes. Perrin plots examining the rotational behavior of the pyrene–Con A complex show good agreement with those previously published for other fluorophore–Con A conjugates. The suitability of this flurorphore as a donor for resonance energy transfer studies is discussed.

Fluorescent ligands have proven to be valuable tools for the study of cell surface topography. The dynamics of receptor redistribution on the cell surface in response to exogenous stimuli or endogenous processes have been most successfully investigated by fluorescence microscopy. The advent of lasers, image intensifiers, and other technological advances (Taylor & Wang, 1980), as well as the increasing availability of fluorescent probes of high specificity, continue to improve the sensitivity and versatility of this approach. The application of resonance energy transfer (RET) techniques to the study of cell surfaces (Fernandez & Berlin, 1976; Chan et al., 1979; Schreiber et al., 1980) have provided a method for quantitating in real time the dynamics of receptor clustering, a phenomenon which appears to be an important step in the initial stages of many cellular responses.

Fluorescent conjugates of lectins and of concanavalin A in particular have been widely used as probes of cell surface architecture and dynamics. Fluorescein and rhodamine derivatives have proven particularly useful. In this paper, we describe the synthesis and some spectroscopic characteristics of a novel fluorescent derivative of Con A.[1] This pyreneacrylate conjugate possesses certain advantages over its fluorescein or rhodamine counterparts, and it is well suited for time-resolved measurements and for RET studies.

We have recently employed this pyrene–Con A derivative as a donor fluorophore (with FITC–Con A as acceptor) in a RET study of the muscle cell surface during myoblast fusion. The results of that investigation are presented in the following paper (Herman & Fernandez, 1982).

Materials and Methods

Synthesis of Pyrene–Con A Conjugates. The FITC conjugate of Con A was prepared according to standard methods. The pyrene conjugate was prepared as follows: 14.9 mg of the succinimide ester of pyreneacrylate (Molecular Probes, Plano, TX) is dissolved in 5 mL of acetone (spectrophotometric grade) to which 100 mg of Celite was added. The solution was evaporated to dryness under a stream of nitrogen. Concanavalin A, 20 mg, was dissolved in 5 mL of 10 mM $NaHCO_3$ with 0.2 M glucose at pH 10.6 and then added to the pyrene–celite adsorbate and stirred on ice for 45 min. After completion of the reaction period, the solution was spun for 15 min at 5000*g* in a Sorvall RC-2B centrifuge to pellet the Celite. The supernatant was dialyzed for 8 h against PBS and then overnight against PBS with Ca^{2+} and Mg^{2+}. The dialyzed solution was layered on top of a 10-cm Sephadex G-50 column. Free pyrene was eluted with a running buffer of 1 M NaCl, 2 mM $MnCl_2$, and 2 mM $CaCl_2$. Labeled Con A was bound to the column. Fluorescence eluted from the column was monitored with a long-wave UV light; after no more fluorescence could be eluted, the labeled Con A was removed by applying a running buffer of 0.2 M glucose. The Con A was collected, dialyzed overnight at 4 °C against phosphate-buffered saline to remove the glucose, and concentrated by vacuum dialysis. The dialysis tubing was prepared by three successive incubations in 0.1, 0.01, and 0.001 M EDTA for 30 min at 100 °C and then stored in 70% ethanol at −15 °C.

The biological activity of the derivatized Con A was tested in 2 ways: First, we performed binding studies with [^{3}H]Con A to examine the efficiency of displacement of [^{3}H]Con A by the fluorescent derivatives and native Con A. Second, myogenic cells were labeled with pyrene- or FITC-conjugated Con A in the presence and absence of 200 mM α-methylmannose (α-MM) and then examined in the fluorescence microscope.

Radioligand Binding Studies with [^{3}H]Con A. Cultured myotubes (see following paper for culture procedure) were harvested for binding assays as follows (Den et al., 1975): Each 35-mm dish was incubated for 10 min with 2 mL of cold (0–4 °C) PBS, pH 7.4. The cells were scraped from the plates and concentrated by centrifugation at 40000*g* for 20 min in a Sorvall RC-5B centrifuge. The supernatant was discarded and the pellet resuspended in an appropriate experimental volume of PBS. Binding reactions were carried out in polypropylene tubes which had been soaked overnight in 0.9% NaCl containing 5 mg of bovine serum albumin (BSA)/mL. The reaction mixture had a total volume of 1.0 mL and contained the following: 1 nM [^{3}H]Con A and appropriate concentrations of Con A, pyrene–Con A, FITC–Con A, *N*-acetyl-D-glucosamine, or α-methylmannoside. The reaction was initiated by addition of 0.5 mL of homogenate. The tubes were incubated for 30 min at 37 °C in a gyrorotatory water bath. The amount of bound ligand was determined with a filtration assay. Nonspecific binding was determined by incubating the radioactive ligand in the presence of 1000-fold excess of unlabeled Con A. Filters were placed in scintillation vials and dried for 1 h under a heat lamp. Econofluor scintillation solution (10 mL) was added to each vial, and samples were counted in a Mark II liquid scintillation counter. Protein

† From the Physiology Department, University of Connecticut Health Center, Farmington, Connecticut 06032. *Received January 12, 1982.* Supported by U.S. Public Service Research Grant GM 23235.

‡ Present address: Anatomy Department, Harvard Medical School, Boston, MA 02115.

[1] Abbreviations: Con A, concanavalin A; EDTA, ethylenediaminetetraacetic acid; PBS, phosphate-buffered saline.

0006-2960/82/0421-3271$01.25/0

concentrations were determined by using the Bio-Rad protein assay.

Spectral Characterization of Con A Conjugates. (*A*) *Spectra.* Absorption spectra for the dye–Con A conjugates were recorded on a GCA McPherson double-beam spectrophotometer with unlabeled protein of the same concentration as a blank. Corrected excitation and emission spectra were obtained with a Perkin-Elmer MPF4 spectrofluorometer equipped with a thermostated sample holder.

(*B*) *Quantum Yields.* Quantum yields were calculated according to (Chen, 1965)

$$Q = Q_q(F/F_q)(A_q/A)$$

where Q is the quantum efficiency of the fluorophore–Con A conjugate, Q_q is the quantum efficiency of a quinine standard solution, A is the absorbance at an appropriate wavelength of fluorophore–Con A conjugate, A_q is the absorbance of quinine at 348 nm, F is the integrated fluorescence intensity of fluorophore–Con A conjugate, and F_q is the integrated fluorescence intensity of quinine.

A value of 0.55 was assumed for the quantum yield of quinine sulfate in 0.1 N H_2SO_4 excited at 348 nm (Chen, 1965). Erroneously low quantum yield values may be obtained due to asymmetric distribution of the emission if the fluorescence viewed at right angles to the exciting light is highly polarized (Singleterry & Weinberger, 1951). Corrections for all the fluorophores employed in our studies were found to be negligible.

Dye to Protein Ratios. Protein concentrations were measured by the method of Lowry (Lowry et al., 1951), and the dye content was assayed spectrophotometrically. From absorbance measurements and knowledge of the molar extinction coefficient, molar dye to protein ratios were calculated. The extinction coefficient, ϵ, for pyrene at 368 is 1.06×10^4 M^{-1} cm^{-1} as measured by us and that of FITC was taken to be 7.2×10^4 M^{-1} cm^{-1} (Chen, 1969).

Fluorescence Polarization. Static polarization measurements were performed with a Perkin-Elmer MPF 4 fluorometer. The polarization, p, was calculated according to

$$p = \frac{I_{VV} - I_{VH}G}{I_{VV} - I_{VH}G} \qquad G = \frac{I_{HV}}{I_{HH}}$$

where I_{VV} and I_{VH} represent the fluorescence intensities (at the wavelength of interest) measured with the analyzer oriented parallel and perpendicular to the vertically polarized excited light and G is an instrumental correction factor. The first and second subscripts refer to the orientation (vertical or horizontal) of the polarizer and analyzer, respectively. Corrections for scattering contributions were performed by subtracting the signals from a similar solution of unlabeled Con A.

Rotational Diffusion Characteristics of Fluorescent Con A Conjugates. For characterization of the rotational freedom of the fluorophore relative to the Con A molecule, Perrin plots of the pyrene–Con A conjugate were obtained. The rotational diffusion of a molecule can be related to its fluorescence polarization by Perrin's equation (Perrin, 1926):

$$\frac{r_0}{r} = 1 + \frac{\tau}{\phi}$$

where ϕ is the rotational correlation time of the molecule, τ is the mean radiative lifetime of the fluorophore, r is the fluorescence anisotropy defined as

$$r = \frac{I_{VV} - I_{VH}}{I_{VV} + 2I_{VH}}$$

and r_0 is the limiting anisotropy corresponding to no motion, as in frozen solution. For a spherical molecule, the rotational correlation time is given by the Einstein–Stokes formula, $\phi = \eta V/(KT)$, where η is the viscosity of the medium, V is the volume of the fluorescent species, K is the Boltzmann constant, and T is the absolute temperature. Perrin plots (a plot of $1/r$ vs. T/η) are useful in determining ϕ and can reveal flexible motions in the protein or local restricted motion of the fluorophore (Wahl & Weber, 1967). Perrin plots were obtained by varying the temperature or by changing the viscosity under isothermal conditions.

Time-Resolved Measurements. Fluorescence decay curves were collected by employing a photon-counting microspectrofluorometer assembled in this laboratory. This apparatus has been previously described (Fernandez & Berlin, 1976; Herman & Fernandez, 1978) and essentially consists of a modified Zeiss research microscope interfaced to an Ortec 9200 nanosecond fluorometer. Deconvolution of decay curves was carried out with the method of moments (Isenberg & Dyson, 1969).

Determination of Critical Forster Radius, R_0, for Pyrene–Fluorescein–Con A. The resonance energy transfer rate from an excited donor (D) to a suitable acceptor (A) in the very weak coupling case under prevailing dipole–dipole interaction (Forster, 1965) is given by

$$K_T = \frac{9(\ln 10)\phi_D\kappa^2}{128\pi^5 N\eta^4\tau_D R^6}J(\lambda) = \frac{1}{\tau_D}\frac{R_0^6}{R}$$

where N is Avogadro's number, η is the refractive index of the medium in the range of overlap, ϕ_D and τ_D are the donor quantum yield and lifetime, respectively, in the absence of acceptor, and κ^2 is an orientation factor defined in terms of the angles between the unit vectors **D**, **A**, and **R** which lie along the donor and acceptor transition moments and the direction joining them, respectively (Dale & Eisinger, 1975). $J(\lambda)$ is the spectral overlap integral of donor (pyrene) emission and acceptor (fluorescein) absorption:

$$J(\lambda) = \int_0^\infty \epsilon(\lambda)f(\lambda)\lambda^4\, d\lambda$$

where $\epsilon(\lambda)$ is the decadic molar extinction coefficient of the acceptor at wavelength λ and $f(\lambda)$ is the normalized fluorescence spectrum of the donor defined as

$$f(\lambda) = \frac{F(\lambda)}{\int_0^\infty F(\lambda)\, d\lambda}$$

where $F(\lambda)$ represents emission intensity per unit wavelength. R_0 is a characteristic distance which is defined as the donor–acceptor separation for which the transfer rate equals the donor deexcitation rate in the absence of acceptor. R_0 is a useful parameter which gives information on the range of D–A separations that can be investigated with a given D–A pair. A value of $^2/_3$ was assumed for τ^2.

Results

Spectral Characteristics. Excitation, emission, and polarization spectra of the pyrene–Con A conjugate in PBS, pH 7.4, are shown in Figure 1. The excitation and emission maxima occur at 373 nm and 463 nm, respectively. The quantum yield for this Con A conjugate is 0.13, and the average molar dye to protein ratio is 2.2.

The binding affinities of pyrene– and fluorescein–Con A conjugates were investigated by a self-displacement binding

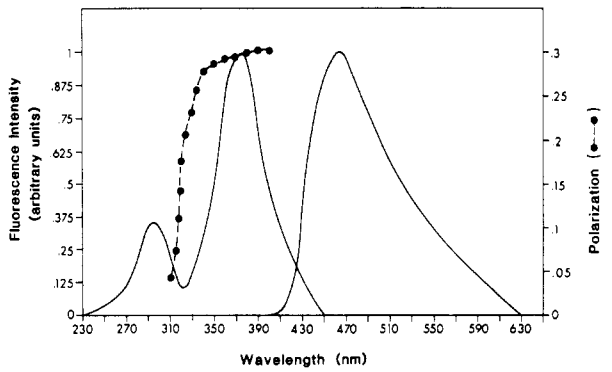

FIGURE 1: Excitation, emission, and polarization spectra of pyrene–Con A. The excitation and emission spectra are normalized to each other at their respective peak intensities. Polarization spectra in 60% sucrose at 2 °C were obtained in a Perkin-Elmer MPF4 by recording the emission of fluorescence at 463 nm while varying the wavelength of excitation. Corrections for depolarization of the emitted fluorescence by the high sucrose were made at each point.

assay: a 1 nM concentration of native Con A caused a 50% inhibition of the binding of 1 nM [^{3}H]Con A to cultured skeletal muscle cells. Pyrene–Con A and FITC–Con A resulted in 42% and 45% inhibition, respectively, at a concentration of 1 nM. Binding specificity of the fluorescent conjugates was verified by examining labeled muscle cells in the fluorescence microscope. In the absence of α-methylmannose, the cells labeled with pyrene–Con A exhibited a blue fluorescence whereas those labeled with FITC–Con A exhibited a yellow-green fluorescence. In the presence of 200 mM α-methylmannose, no fluorescence was visible.

The fluorescence decay behavior of pyrene–Con A is shown in Figure 2. The results of a single-exponential fit to the data are shown in Figure 2A, whereas those of a two-component analysis are shown in Figure 2B. It is clear that pyrene–Con A does not decay with first-order kinetics. Analysis of the residuals, however, shows that a two-component analysis (τ_1 = 21.0 ns, τ_2 = 2.99 ns; α/α_2 = 0.045) provides an adequate description of the decay. The origin of the double-exponential decay of pyrene–Con A is not clear. In principle, this behavior could be caused by oxygen quenching of the emission, by heterogeneity in binding to Con A, by excimer formation, or by other intramolecular photophysical processes.

One initial concern was the possibility that some of the emission may have arisen from excimers, particularly in view of the well-known ability of pyrene to form excimers (Alwatter et al., 1973) and the fact that the emission spectrum of pyrene–Con A (a broad structureless envelope peaking at 463 nm) resembles that of pyrene excimer more than that of the monomer. The latter exhibits pronounced vibronic structure and peaks at about 383 nm. For clarification of this point, excitation and emission spectra of pyreneacrylate conjugated to diethylamine were taken over a range of concentrations. While the excitation spectrum did not change with concentration, the emission spectrum developed a new band at 508 nm at higher concentrations. Figure 3 shows emission spectra from one of these experiments at 1.0 μM and 1.0 mM concentrations. This behavior is characteristic of excimer formation. Sice the pyrene–Con A emission corresponds to that found for the pyreneacrylate–diethylamine conjugates at low concentrations, we have ruled out excimer formation as a contributing factor to the double-exponential decay kinetics of pyrene–Con A.

For an investigation of a possible role for oxygen quenching in the decay characteristics of pyrene–Con A, decay curves were collected from aerated samples and from samples purged

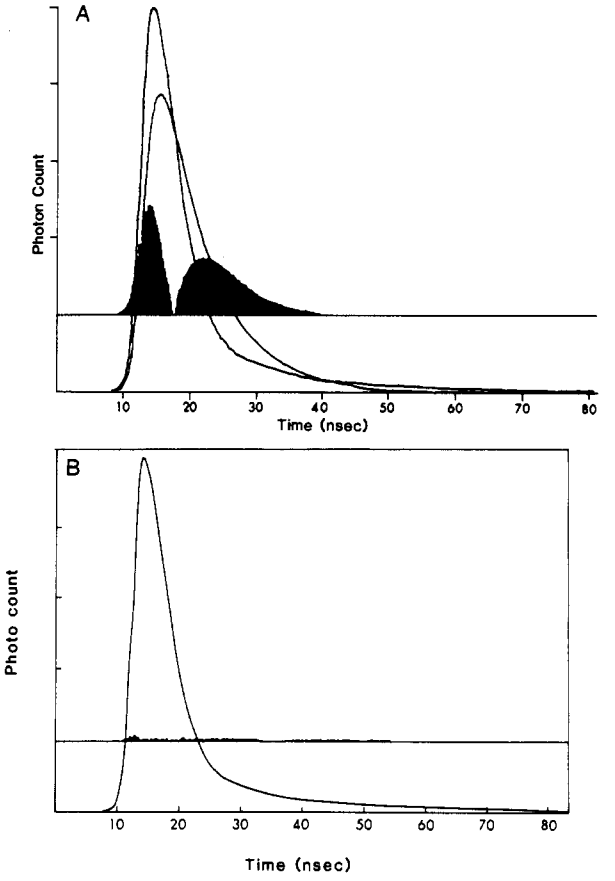

FIGURE 2: Fluorescence decay of pyrene–Con A (1×10^{-6} M protein) in PBS, pH 7.4 at 22 °C. (A) Superposition of experimental and calculated (top curve) fluorescence decay curves obtained from a one-component deconvolution. (B) Superposition of experimental and calculated fluorescence decay curves obtained from a two-component deconvolution. Residuals are also shown. The excitation and fluorescence curves were collected to 100 000 and 20 000 in their peak channels, respectively. Data were collected from a sample of Con A which was placed in a well slide on the stage of the microscope.

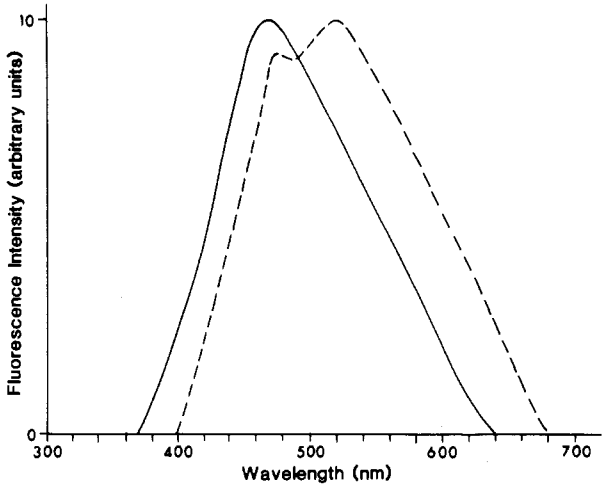

FIGURE 3: Emission spectra of pyreneacrylate conjugated to diethylamine. The solid line represents pyreneacrylate at a concentration of 1 μM and the dotted line represents pyreneacrylate at a concentration of 1 mM.

with nitrogen. The decay curves were similar in both cases, suggesting that oxygen quenching is not a significant factor in the genesis of the double-exponential behavior.

To clarify the role of binding heterogeneity, we first investigated the effect of solvent environment on the spectral characteristics of the free pyreneacrylate. Table I summarizes

Table I: Spectral Properties of Pyreneacrylate Succinimide Ester in Different Solvents[a]

solvent	λ_{ex}	λ_{em}	Q
water	380	532	0.16
ethanol	378	500	0.33
acetone	370	470	0.35
xylene	383	445	0.29

[a] Dye concentration was 1 μM in all cases.

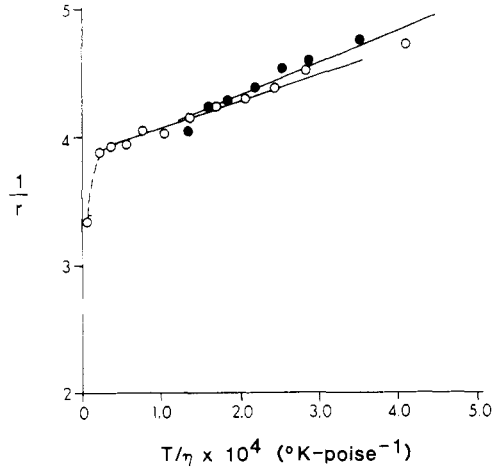

FIGURE 4: Perrin plot ($1/r$ vs. T/η) of pyrene–Con A. The concentration of pyrene was 1×10^{-6} M, and the molar dye/protein ratio (D/P) was 2.2:1. (Open symbols) Isothermal run, where the viscosity is altered by varying the percentage of sucrose (5–60% w/w) in the solution. (Closed symbols) A "heat run", where the sucrose concentration is held constant (10% w/w) and the temperature is altered. The dotted line shows values at very low T/η corrected for depolarization of the emitted fluorescence due to scatter from the sucrose molecules in the solution.

these results. It can be seen from this table that the excitation maximum does not change appreciably but that the emission maximum displays marked sensitivity to environment, shifting from 532 nm in water to 445 nm in xylene. This might suggest that heterogeneity in binding to Con A may lead to the decay kinetics observed. To further test this possibility, we conjugated pyreneacrylate to a small free amine (diethylamine). The reaction was carried out in an excess of diethylamine to ensure complete conjugation of the acrylate and thus a homogeneous population of emitting species. At 1 μM concentration, the excitation and emission maxima of this conjugate were 375 and 463 nm, respectively, in close agreement with the values of these parameters for pyrene–Con A. Interestingly, the decay kinetics of this homogeneous population of fluorophores were comparable to those of pyrene–Con A. This evidence suggests that heterogeneity in binding site environments is not responsible for the two-exponential decay of pyrene–Con A.

Perrin Plots. Figure 4 shows a Perrin plot of pyrene–Con A. The open circles represent an isothermal Perrin plot (the temperature is held constant while the viscosity is changed), and the closed circles represent a "heat run" (the temperature is varied at constant sucrose concentration). This figure shows a behavior typical of the case where the fluorescence depolarization is caused by two distinct rotations: a relatively fast hindered rotation of the fluorophore about the bond of attachment to the protein and a relatively slow rotation of the protein molecule (Wahl & Weber, 1967). The relative contributions of each of these motions to the fluorescence depolarization depend on both T and η. At low T/η values, rotational motion of the entire protein occurs on a much slower time scale than that of the excited state lifetime; thus the

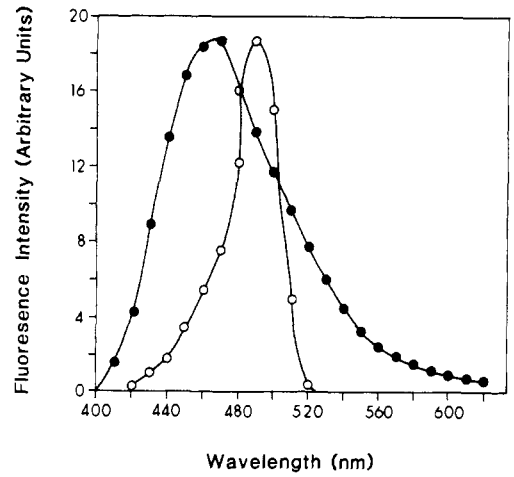

FIGURE 5: Spectral overlap between the emission of pyrene–Con A and the absorption of FITC–Con A. The two spectra are normalized at their respective peak intensities. The overlap integral is calculated as described under Results. The closed symbols represent the emission spectrum of pyrene–Con A, and the open symbols represent the absorption spectrum of FITC–Con A.

fluorescence depolarization seen is caused predominantly by local motion of the fluorophore. At high T/η values, orientational relaxation of the fluorophore occurs rapidly relative to the excited state lifetime, so that the changes in polarization reflect only the rotations of the protein molecule.

Our results with pyrene–Con A are similar to those previously obtained in Inbar et al. (1973) with FITC–Con A. In this case the linear region of the isothermal curve extrapolates to an R_0 value of 0.26. Employing this value in Perrin's equation (at $T/\eta = 2.86 \times 10^4$ K P^{-1}) and a lifetime of 2.99 ns (the fast component that accounts for about 96% of the total signal), we obtain a rotational correlation time, ϕ, of 16.3 ns. This value is in reasonable agreement with the previously reported value of 19.3 ns for FITC–Con A (Inbar et al., 1973). Decay of anisotropy curves (data not shown) suggests that the correlation time for the local restricted motion of the pyrene moiety is less than 0.5 ns.

R_0 Values. The value of R_0 was calculated according to

$$R_0 = [(8.785 \times 10^{-25})\kappa^2 Q \eta^{-4} J(\lambda)]^{1/6}$$

where the variables assume the same meaning as under Materials and Methods.

Figure 1 is a graph of the excitation and emission spectra of pyrene–Con A. These spectra show some overlap and yield an R_0 for pyrene–pyrene self-transfer of 22 Å. The overlap between the pyrene emission and the fluorescein absorption is shown in Figure 5. The R_0 value for this pair is 43 Å.

Discussion

Our choice of a pyrene fluorophore to label the Con A molecule was guided by our interest in a probe that (a) could be efficiently excited at 380 nm and (b) would serve as an effective donor to fluorescein–Con A derivatives in RET experiments.

The first of these two requirements is related to our interest in performing time-resolved studies on single cells for which we employ an air-gap discharge flash lamp as an excitation source. The spectral output of these lamps is limited to several discrete bands in the UV, with most of their output centered around 360 and 380 nm and little or no output in the visible. The excitation peak of pyrene–Con A (Figure 1) closely coincides with 380-nm emission of the nitrogen discharge. This provides efficient excitation of the probe and good signal-to-

noise ratios and permits collection of decay curves from single cells in reasonably short times.

The suitability of this probe to serve as a donor to fluorescein (FITC) in RET experiments can be seen from Figure 5 which shows the spectral overlap between pyrene emission and fluorescein absorption. The R_0 for the pyrene–fluorescein pair is 43 Å which is sufficiently large to make this donor–acceptor combination useful for studies of cell surface receptor clustering [see following paper (Herman & Fernandez, 1982)]. In addition, the large Stokes shift of the pyrene fluorescence results in little self-overlap between pyrene's own emission and absorption bands. Thus, the R_0 for pyrene–pyrene self-transfer is only 22 Å (compare to 48 Å for fluorescein self-transfer). This constitutes an additional advantage of employing pyrene as a donor, since potential artifacts due to donor self-transfer are significantly reduced. Finally, the rapid local relaxation of the pyrene moiety relative to the Con A molecule and the fact that there is little direct excitation of fluorescein at the excitation maximum of the pyrene further add to the usefulness of this pyrene–Con A derivative as a probe for resonance energy transfer studies.

References

Alwattar, A. H., Lumb, M. D., & Birks, J. B. (1973) in *Organic Molecular Photophysics* (Birks, J. B., Ed.) p 447, Wiley, New York.

Chan, S. S., Arndt-Jovin, D. J., & Jovin, T. M. (1979) *J. Histochem. Cytochem. 27*, 56.

Chen, R. F. (1965) *Science (Washington, D.C.) 150*, 1593.

Chen, R. F. (1969) *Arch. Biochem. Biophys. 133*, 263.

Dale, R. E., & Eisinger, J. (1975) in *Biochemical Fluorescence: Concepts Volume 1* (Chen, R. F., & Edelhock, H., Eds.) p 120, Marcel Dekker, New York.

Den, H., Malinzak, D. A., Keating, H. J., & Rosenberg, A. (1975) *J. Cell Biol. 67*, 826–834.

Fernandez, S. M., & Berlin, R. D. (1976) *Nature (London) 264*, 411.

Forster, T. (1965) in *Modern Quantum Chemistry* (Sinagolu, O., Ed.) Part III, Academic Press, New York.

Herman, B. H., & Fernandez, S. M. (1978) *J. Cell. Physiol. 94*, 253.

Herman, B. A., & Fernandez, S. M. (1982) *Biochemistry* (following paper in this issue).

Inbar, M., Shinitzky, M., & Sachs, L. (1973) *J. Mol. Biol. 81*, 245.

Isenberg, I., & Dyson, R. (1969) *Biophys. J. 9*, 1337.

Lowry, O. H., Rosenbrough, N. J., Farr, A. L., & Randall, R. J. (1951) *J. Biol. Chem. 193*, 256.

Perrin, F. J. (1926) *J. Phys. Radium 7*, 390.

Schreiber, A. B., Hoebeke, J., Vray, B., & Storsberg, A. D. (1980) *FEBS Lett. 111*, 303.

Singleterry, C. R., & Weinberger, L. A. (1951) *J. Am. Chem. Soc. 73*, 4574.

Taylor, D. L., & Wang, Y.-L. (1980) *Nature (London) 284*, 405–410.

Wahl, P., & Weber, G. (1967) *J. Mol. Biol. 30*, 371.

Dynamics and Topographical Distribution of Surface Glycoproteins during Myoblast Fusion: A Resonance Energy Transfer Study†

Brian A. Herman‡ and Salvador M. Fernandez*

ABSTRACT: We have investigated changes in topography and lateral translational mobility of concanavalin A (Con A) receptors on the surface of cultured chick muscle cells during the period of myoblast fusion. A temporal correlation between these phenomena and the alteration in membrane fluidity known to occur during this time period is established. Receptor topography and mobility are studied by means of a resonance energy transfer technique employing pyrene- and FITC–Con A conjugates. All measurements are performed through a microscope on single cells. Our results reveal that during the period of myoblast fusion Con A receptors undergo a dramatic redistribution on the cell surface. Furthermore, our data suggest that the changes in membrane fluidity observed during muscle differentiation serve to modulate the lateral mobility of these receptors.

One of the earliest events in the process of muscle differentiation is the fusion of myoblasts into multinucleated myotubes. This phenomenon has been the subject of a great deal of attention not only because of its fundamental importance as a developmental process but also because it provides a good model for the study of membrane fusion in general. A number of observations now indicate that cell surface lectins and the lipids of the plasma membrane play important roles in the process of myoblast fusion. Lectins, on the one hand, are envisaged as serving a function in cellular recognition and adhesion (Rosen et al., 1975) while membrane lipids, on the other hand, are considered to be more intimately involved with the fusion event proper (Horwitz et al., 1979; Kalderon & Gilula, 1979).

Several lines of evidence have implicated lectins in the process of myoblast fusion. First, cultured muscle cells elaborate surface lectins as a prelude to fusion activity (Gartner & Podleski, 1976; Nowak et al., 1976; Teichberg et al., 1975). Second, exogenous addition of certain lectins to myogenic cultures results in marked inhibition of fusion (Den et al., 1975; Sandra et al., 1977). More recently (Parfett et al., 1981) it has been shown that Con A[1] resistant myoblast lines defective in their ability to synthesize surface mannosylated glycoproteins do not undergo fusion. Suggestions for a lipid in-

† From the Physiology Department, University of Connecticut Health Center, Farmington, Connecticut 06032. *Received January 12, 1982.* Supported by U.S. Public Service Research Grant GM 23235.

‡ Present address: Anatomy Department, Harvard Medical School, Boston, MA 02115.

[1] Abbreviations: Con A, concanavalin A; EGTA, ethylene glycol bis(β-aminoethyl ether)-*N,N,N',N'*-tetraacetic acid.

0006-2960/82/0421-3275$01.25/0